CONF-8909238--1

DE90 001346

ITER PHYSICS R & D PROGRAMME

PROGRESS REPORT FORM

DATE: September 30, 1989

PAGE 1 /1

TASK TITLE: Alpha particle losses induced by the toroidal magnetic field ripple

ORGANIZATION: Oak Ridge National Laboratory

DEVICE: ATF

END OF REPORTING PERIOD September 30, 1989

PLEASE REFER TO THE TASK PHASES OF THE TASK DEFINITION FORM

SUMMARY OF RESULTS:

We have used the usual axisymmetric equilibrium + vacuum ripple model to study alpha losses at low energy. Previous ITER studies have shown that alpha losses near the birth energy are small. Since there is very little pitch angle scattering above E_{crit}, this situation should pertain above this energy. Below E_{crit}, pitch angle scattering increases and the alpha particles have another opportunity to find the ripple and 1/R loss regions. Accordingly, we have started 1000 alpha particles at their local E_{crit}, and followed them in real space until they thermalize. About 6% of the alphas are lost with an energy that is only 0.6% of the initial 3.5 MeV energy.

With respect to task PH12-US, we have not yet succeeded in obtaining a fully-converged 3-D free-boundary VMEC equilibrium for ITER. If the boundary is allowed to remain free for some period of time and then is fixed, the code converges well. Otherwise, it does not converge as well as we would like. For the cases where the boundary was frozen after the code had partially converged, the rippled equilibrium did not show any especially pathological properties. Current efforts are directed at improving the temporal convergence of VMEC by application of a preconditioning algorithm and by improving the basic time-stepping procedure. These modifications have already led to substantial improvement in fixed boundary calculations. Within the next few weeks, the revised code will be applied to the free-boundary ITER case.

ENCLOSURES

TF-Ripple Losses of Suprathermal Alphas in ITER by L. M. Hively and J. A. Rome, Oak Ridge National Laboratory.

REFERENCES OF RELATED REPORTS OR PUBLICATIONS

Research sponsored by the Office of Fusion Energy, U.S. Department of Energy, under contract DE-AC05-84OR21400 with Martin Marietta Energy Systems, Inc.

TF-Ripple Loss of Suprathermal Alphas in ITER

L.M. Hively and J.A. Rome
Fusion Energy Division
Oak Ridge National Laboratory
Oak Ridge, TN 37831-8071

ABSTRACT

TF-ripple loss of alphas below the critical energy is calculated for a non-circular ITER plasma. For 14 toroidal field (TF) coils, the particle loss was found to be about 6%. About 0.6% of the initial alpha energy (3.5 MeV) is lost.

I. INTRODUCTION

Alpha particle losses, induced by toroidal field (TF) ripple, have an important impact on the overall tokamak reactor design, including the TF coils, first wall, and divertor. High alpha loss would reduce the alpha heating of the plasma and even could preclude ignition. Wall damage by a high alpha flux could increase plasma impurities, with a corresponding reduction in plasma energy confinement. Therefore, careful analysis of alpha ripple losses is needed.

Recent calculations of TF-ripple loss of alphas in ITER were presented at an IAEA-sponsored experts' meeting [1]. For the ITER physics phase plasma (22 MA, 16 TF coils with 1.5% outboard ripple), the alpha power loss fraction was calculated to be less than 1% [2-4]. The corresponding wall heat flux is well below the allowable limit. However, these calculations addressed only the loss of MeV alphas. If we assume that any trapped high energy alphas that are going to be lost due to ripple effects are lost fairly quickly, the next opportunity for losses will occur after the alphas have slowed down to the critical energy. Below the critical energy (≤800 keV in ITER, see Fig. 1), pitch angle scattering can repopulate any loss region and may cause additional loss of the fast alpha particles. The behaviour of the alpha particles from the critical energy to thermalization at $\frac{3}{2}kT_i$ is the subject of this paper.

The outline of this work is as follows: The Monte Carlo model used to follow orbits is presented in Sec. II. Our results are discussed in Sec. III, followed by conclusions in Sec. IV.

II. ALPHA LOSS MODEL

A Monte-Carlo, guiding-center model chooses the fast alphas and follows the collisionless orbits. Alphas are thermalized and scattered in pitch angle after each collisionless time step, and followed to a minimum (thermal) energy. Table 1 summarizes the model, together with references for further details.

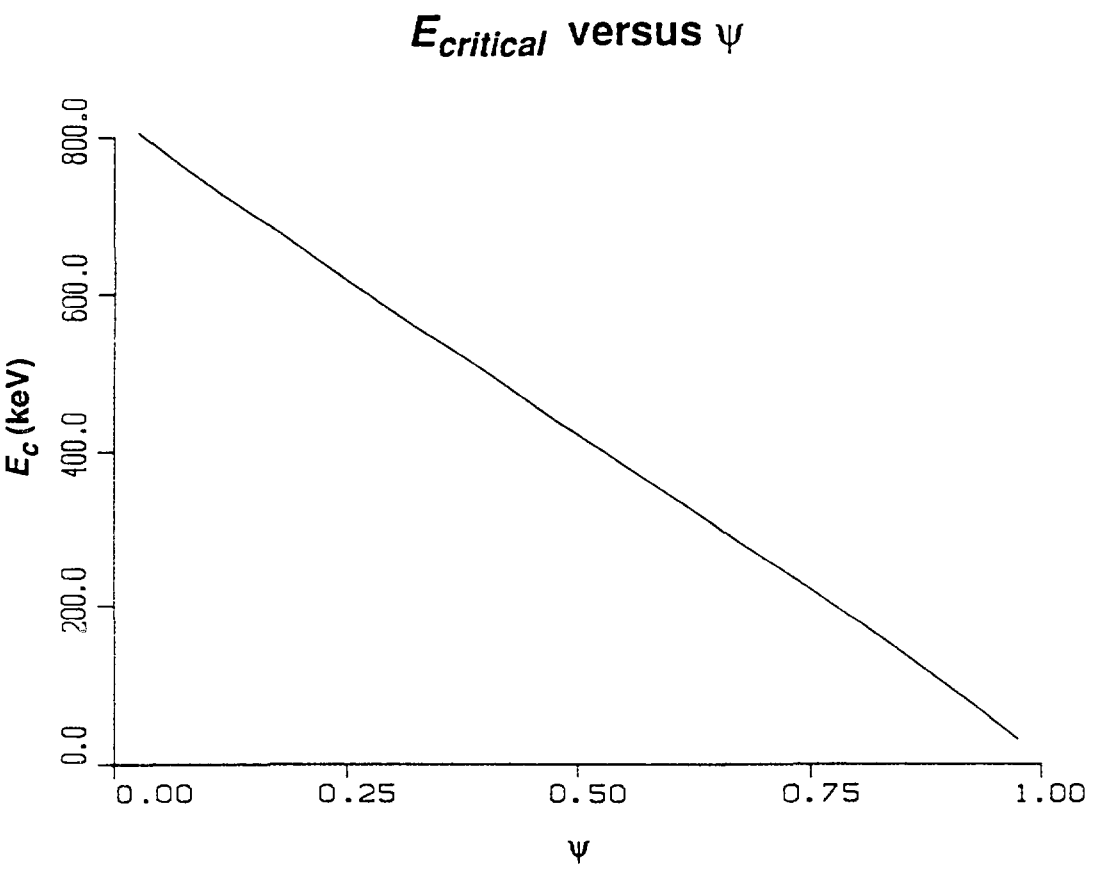

Figure 1: Thermalizing alpha particles transfer energy equally to the background ions and electrons at the critical energy, E_c. Since pitch angle scattering is negligible above E_c, the alpha particles were born with an energy E_c on each flux surface.

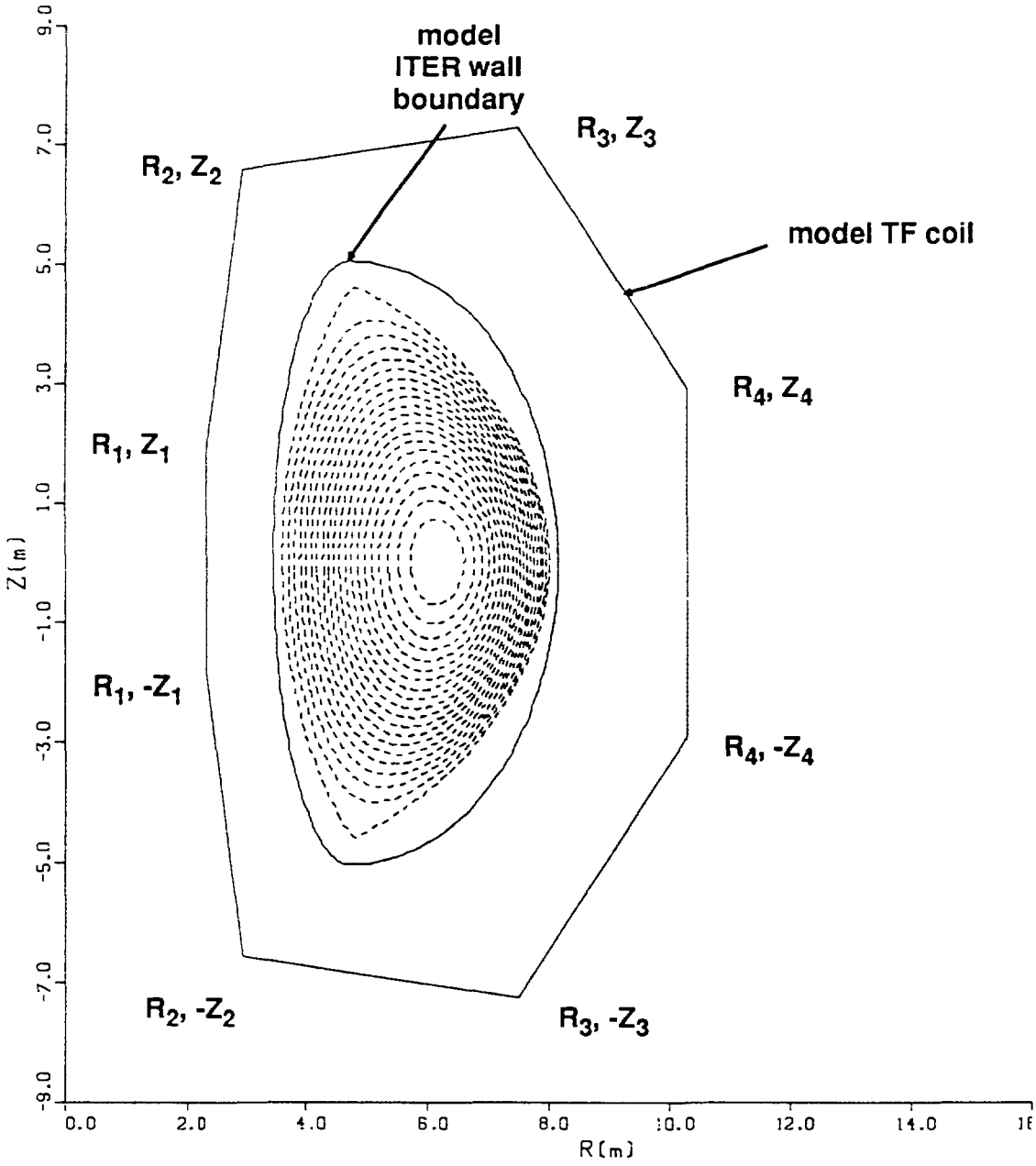

Figure 2: The 2-D ITER equilibrium used in these calculations as provided by Strickler [7]. The models for the ITER wall and the 8 wire segment TF coils are shown. The coordinate values for the coil filaments are given in Table 2.

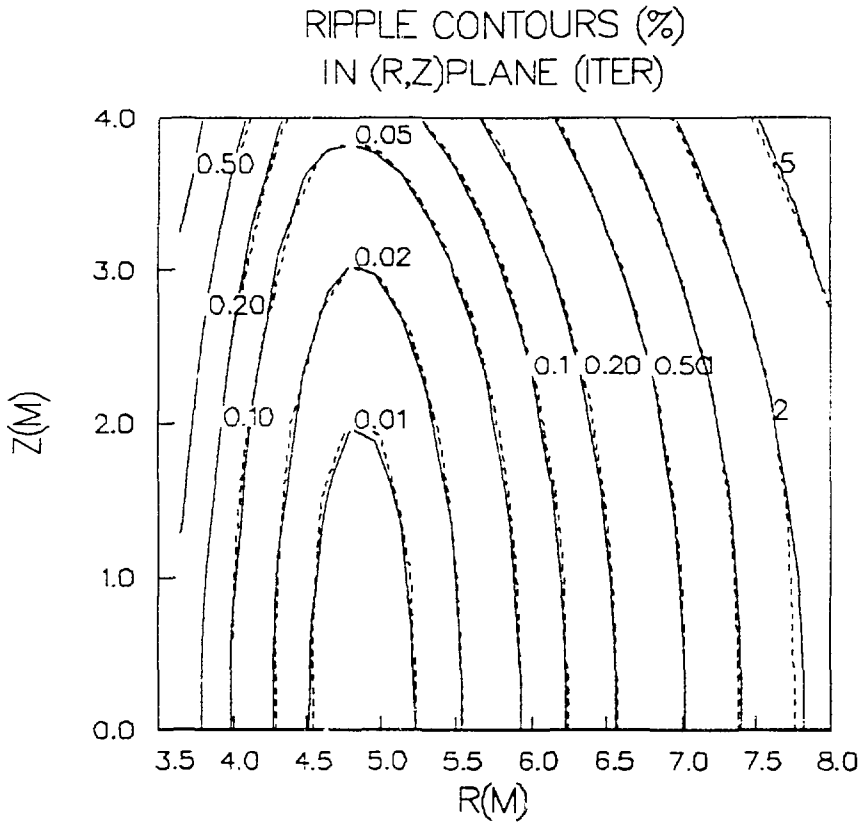

Figure 3: The ITER TF ripple contours (solid lines) and the ripple contours from the 8 wire segment model of Figure 2.

Several aspects of the model are noteworthy. In this paper, the magnetic field is modeled as the sum of the axisymmetric (2D) equilibrium and the TF ripple field, even though the actual 3D field arises from a 3D rippled equilibrium which should be calculated self-consistently. Johnson and Reiman [12] found that the plasma current flowing along rippled field lines in INTOR increases the ripple by a factor of 1.4–1.5 at finite beta implying that a 3D rippled equilibrium model is needed for ITER. A free-boundary, finite beta, 3D rippled equilibrium model is the subject of other work but is not yet complete[13].

The vacuum ripple field is calculated from the Biot-Savart law with each of the (N=14) TF coils consisting of 8 straight, filamentary wires (see Fig. 2). This filamentary model was used instead of the finite cross-section TF coils to make the calculation possible in a reasonable amount of computer time. The minimum number (14) of TF coils was used to exacerbate any ripple-produced effects. The end points of the wire segments (see Table 2) are found by minimizing the fractional difference between the calculated ripple and ITER ripple data[16] as shown in Fig. 3. The Littlejohn form [14] of the guiding center equations is used to follow the alpha orbits [15].

The wall can be modeled by the form [10]:

$$R = R_{sep} + a_1 \cos(\theta) \qquad -\frac{\pi}{2} \le \theta \le \frac{\pi}{2}$$

$$= R_{sep} + a_2 \cos(\theta) \qquad \frac{\pi}{2} \le \theta \le \frac{3\pi}{2}$$

$$Z = b\sin(\theta)\,,$$

where

$$a_1 = R_0 + a + s - R_{sep}$$
$$a_2 = R_{sep} - (R_0 - a - s)$$
$$b = Z_{sep} + 2.5s$$
$$\theta = \text{poloidal angle}$$

The remaining notation is standard and is summarized in Table 3 along with other ITER parameters [8]. The collisional effects due to speed diffusion and a toroidal electric field are unimportant [5-6] and are not included in these calculations. Thermalization and pitch angle scattering on impurities are included via the factors, $\langle Z \rangle$ and [Z], which are defined by

$$\langle Z \rangle = \sum_i n_i Z_i^2 / n_e \qquad (1)$$

$$[Z] = \sum_i n_i Z_i^2 / (A_i n_e) \tag{2}$$

For the i^{th} ion species, the symbols are density (n_i), charge (Z_i), and atomic number (A_i); the electron density is n_e. The ITER reference parameters assume the following impurities: 5% thermalized alphas, 1.5% carbon, 0.5% oxygen and 0.05% iron; equal fractions of deuterium and tritium are used [17]. The resulting values for $\langle Z \rangle$ and $[Z]$ are as shown in Table 3. The fraction, f_H ($\equiv n_H/n_e$), of hydrogenic species (deuterium + tritium) is 0.757 as obtained from the charge quasi-neutrality condition:

$$1 = \sum_i n_i Z_i / n_e \tag{3}$$

However, our model can handle only a single impurity species which we take as having charge Z_I and mass number A_I. Solving Eqs. (1) and (3) for Z_I yields

$$Z_I = \frac{\langle Z \rangle - f_H}{1 - f_H} \tag{4}$$

The corresponding fractions for the equivalent single impurity, f_I, and the hydrogenic species are

$$f_I = \frac{\langle Z \rangle - 1}{Z_I(Z_I - 1)} \tag{5}$$

$$f_H = \frac{Z_I - \langle Z \rangle}{Z_I - 1} \tag{6}$$

Substituting Eqs. (5)-(6) into (2), yields an expression for A_I:

$$A_I = \frac{Z_I(\langle Z \rangle - 1)}{[Z](Z_I - 1) + \frac{5}{12}(\langle Z \rangle - Z_I)} \tag{7}$$

For $f_H = 0.757$, $\langle Z \rangle = 2.15$, $[Z]$=0.44, the resulting single-impurity parameters are, from Eqs. (4)-(7): $Z_I = 5.75$, $A_I = 11.22$, $f_I = 4.22\%$; these last values were used for the alpha loss simulations.

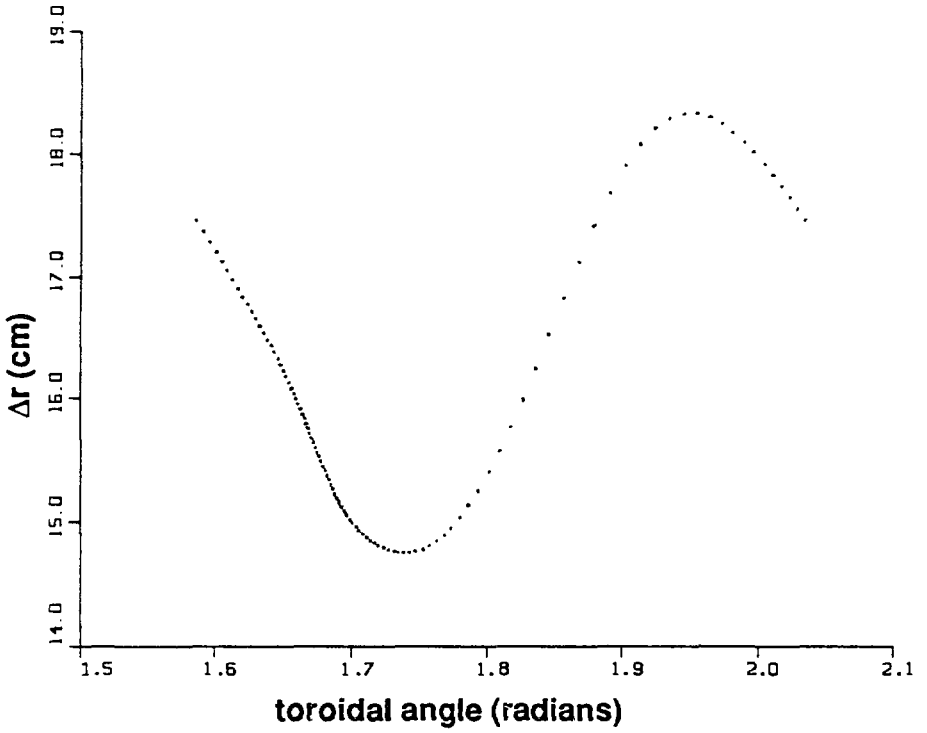

Figure 4: The variation of the collisionless banana width as a function of the toroidal location of the intervening banana tip. The smoothness of the data and agreement with Eq. 8 demonstrates the accuracy of integration scheme used in this paper.

III. RESULTS

We first comment on the properties of single-particle collisionless alpha orbits in a rippled tokamak. For finite banana-width orbits, the variation in banana width, Δr, versus the toroidal position, φ, of the intervening banana tip takes the form

$$\Delta r = \sum_{i=0}^{m} d_i \cos(iN\varphi_t + \varphi_i) + d_c \tag{8}$$

The first two terms in the Fourier series on the RHS correspond to the small banana-width expression obtained by Boozer [18]. The additional terms in the Fourier series provide an excellent fit to the variation for a collisionless, large banana-width orbit in a noncircular tokamak (RMS error $\sim 10^{-4}$). Fig. 4 shows an example for a 3.5 MeV alpha in ITER, and demonstrates the accuracy of our integration technique. The last term on the RHS of Eq. (8) depicts pitch angle scattering, too small to be displayed in Fig. 4, which overwhelms the high order harmonics. The collisional term describes pitch angle scattering as a random variable with zero mean, having a normal distribution with a standard deviation that depends on the starting point in phase space [19].

The simplest form of Eq. (8) [20] and improvements on that form (e.g., Refs. 21-24) have been used by others as a mapping method to follow stochastic ripple loss of alphas. However, pitch angle scattering is small compared to thermalization for MeV alphas. A better form of this mapping in noncircular plasma uses the constants-of-motion (COM) formulation developed by Rome and Peng [25] to include the collisionless variation in the banana width as well as pitch angle scattering and slowing-down:

$$\Delta\psi_m = \psi_C + \sum_{i=0}^{m} \psi_i \cos(iN\varphi + \varphi_i) \tag{9}$$

$$\Delta\zeta = \zeta_C \tag{10}$$

$$\Delta v = v_C \tag{11}$$

Without ripple, each orbit is specified by the ion speed (v), the maximum value of the poloidal flux coordinate along the orbit (ψ_m), and the cosine of the pitch angle (ζ) at ψ_m. With ripple, the value of toroidal angle (φ) at ψ_m is needed to uniquely specify the orbit. The above equations specify the mapping over one bounce period. In Eqs. (9)–(11), the change in each quantity due to collisions is denoted by the subscript C. Without pitch angle scattering, the collisional terms can be approximated by $x_C = (dx/dt)\tau_b$, where x corresponds to each of the variables in Eqs. (9)–(11), and τ_b is the banana bounce period for an axisymmetric orbit. The expressions for dx/dt were obtained analytically by Hively et al.[26] without pitch angle scattering for an axisymmetric tokamak. With pitch angle scattering in a rippled tokamak, the collisional terms must be calculated numerically over the 4D phase space (v, ζ, ψ_m, φ). This phase group analysis is beyond the scope of the present work, but would be much faster than the detailed guiding center orbit following with collisions, as discussed next.

We performed a 1000-particle simulation of alpha thermalization in a rippled ITER equilibrium via guiding-center orbit following requiring more than 16 hours of Cray computer time. The details of the initial alpha distribution are listed in Table 1. On each flux surface, the alpha particles were launched at the local value of the critical energy as shown in Fig. 1. Alphas hitting the wall during the first bounce period (prompt lost) were rejected since they would presumably have been lost at much higher energy. During the time that the alpha particles are in circulating orbits, it is legitimate to enhance the slowing down process. The scattering was done by performing 200 small-angle collisions after each orbit integration step instead of only one small-angle collision without enhancement, or one collision enhanced 200-fold as was done in [5]. As soon as the orbit's parallel velocity dropped to zero, the acceleration was discontinued

so that the full effect of ripple on the banana-trapped orbits was taken into account.

To illustrate the thermalization and pitch angle scattering process, Fig. 5 shows the orbits of 100 alpha particles in ψ–ζ space.

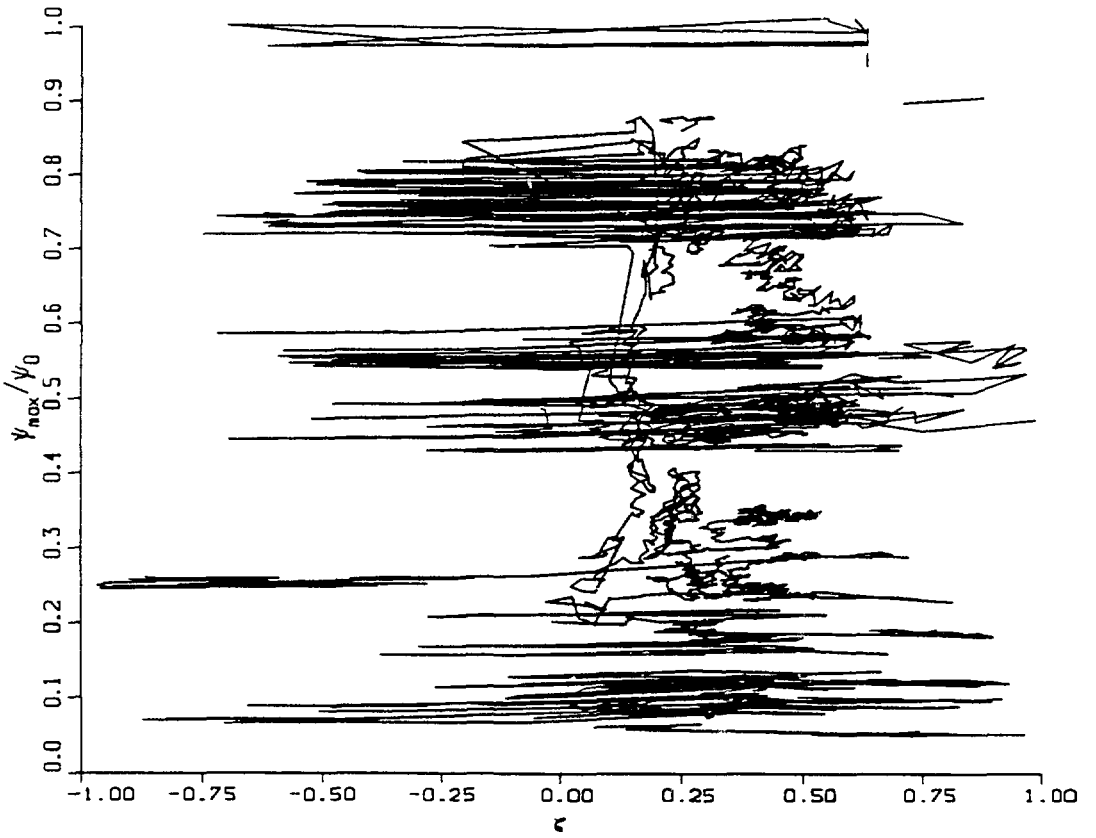

Figure 5: The normalized flux surface versus pitch angle for 100 alpha particles as they slow down from E_c to $\frac{3}{2}\, kT_i$.

IV. CONCLUSIONS

Losses during the thermalization of alphas from the critical energy (800 keV) to thermal energy (50 keV) are small in ITER as determined by a 1000-particle simulation via guiding center following and Monte Carlo scattering. Figure 6 shows the birth points of the particles in (ζ, ψ_m) space. The birth points of the lost alphas are shown in Fig. 7. The birth distribution in this space should not be uniform since the Jacobean in this space depends upon the bounce time. The points with both square and round symbols correspond to particles for which $v_{||}$ goes to zero along the orbit.

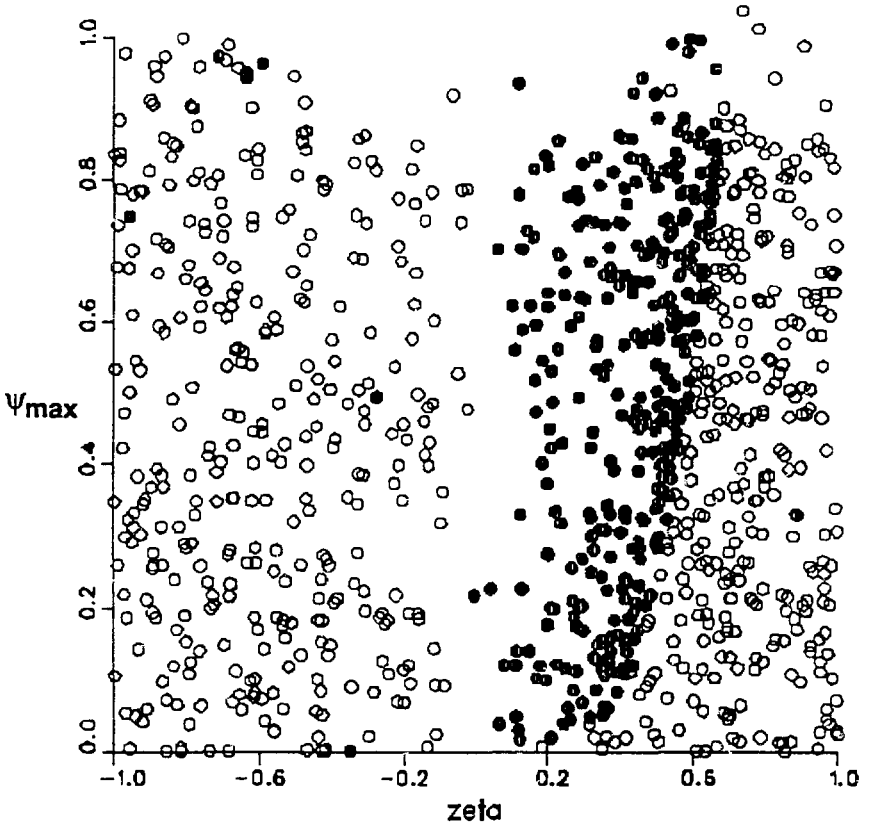

Figure 6: The birth points of alpha particles at the local value of E_{crit} in $\psi_{max} - \zeta$ space. The dark symbols mean the particle is trapped.

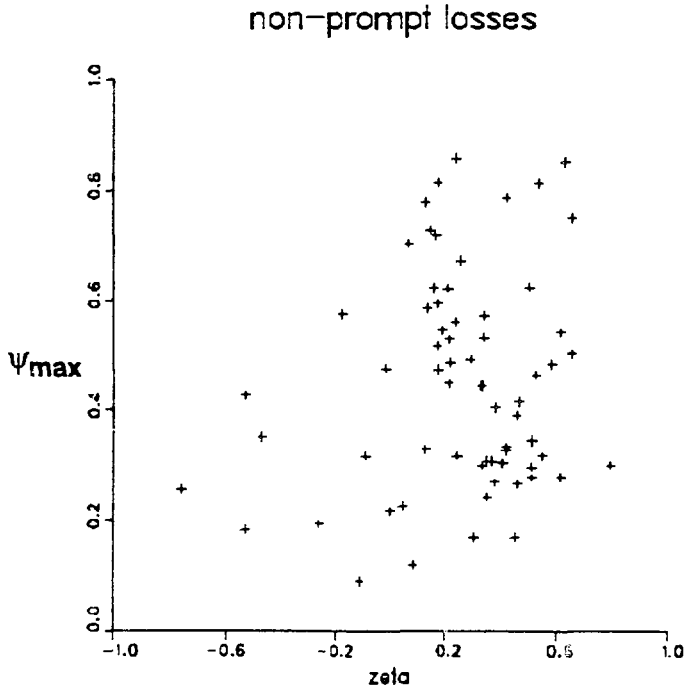

Figure 7: The birth points of the lost alpha particles

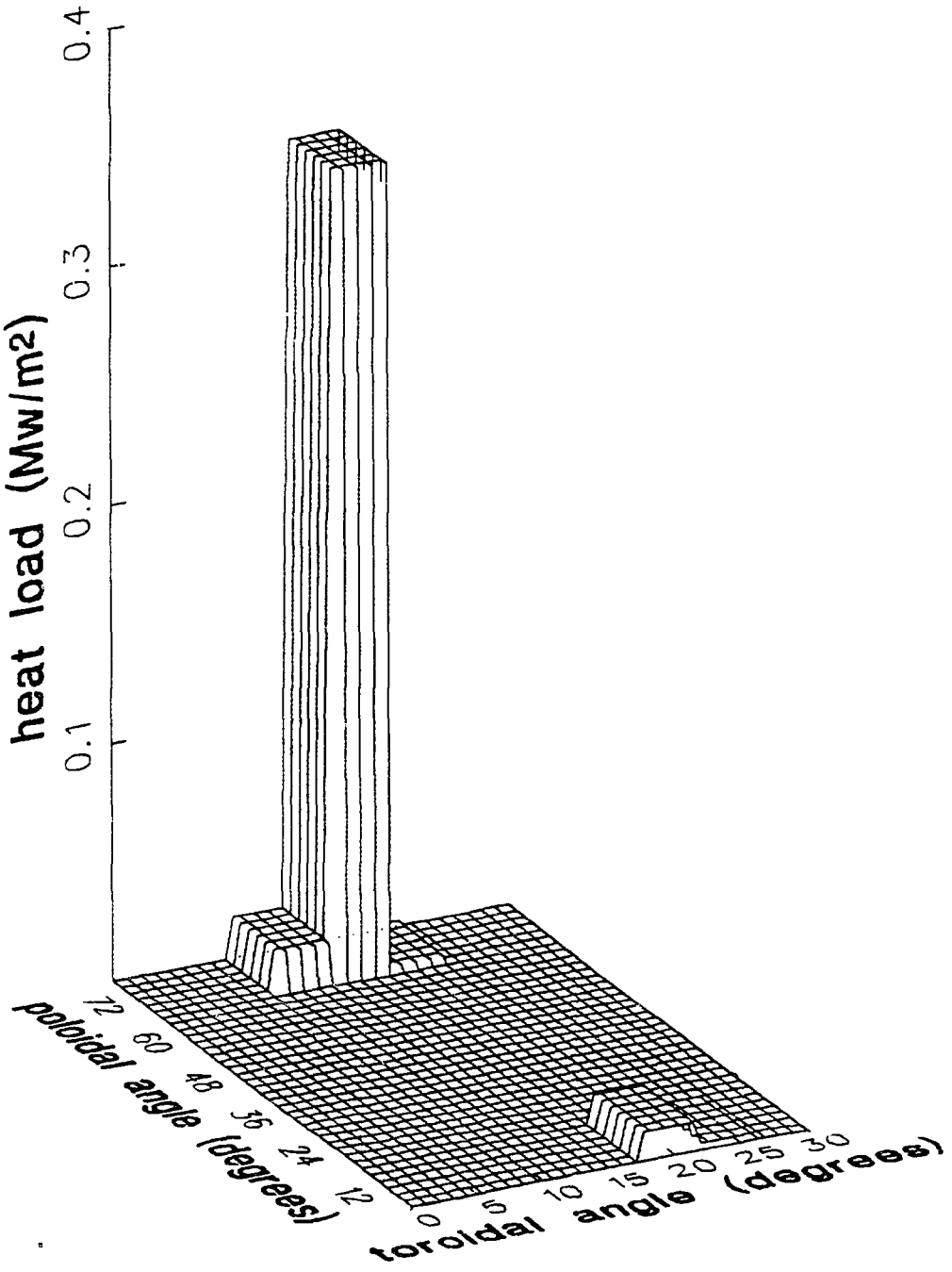

Figure 8: The wall-loading due to alpha particles as they thermalize at energies below E_{crit}. All losses have been plotted in one field period.

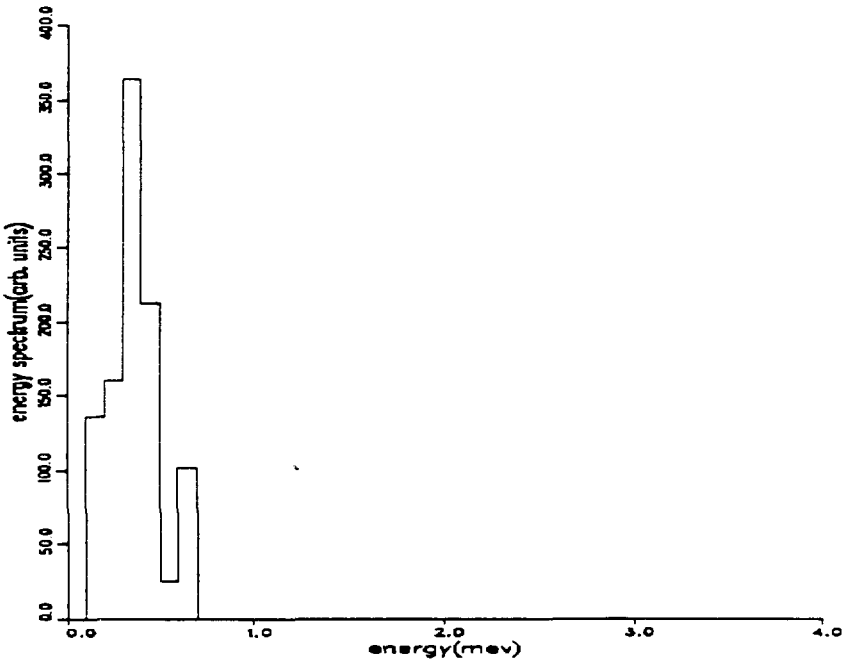

Figure 9: The energy spectrum of alpha particles that hit the wall at energies below E_{crit}.

The fraction of the initial 3.5 MeV energy that was lost was only 0.61% ± 0.01%. The fraction of particles which hits the wall was 5.99% ± 0.07%. Therefore, any wall-loading due to alpha particles in ITER can be adequately modeled with the previous high energy results. The distribution of these losses on the wall is shown in Figure 8. The losses are concentrated near the equator and near 70°. The former are probably due to the outward diffusion of circulating orbits, and the latter are probably due to the upward drift of ripple-trapped alphas. The energy spectrum of the lost particles is shown in Fig. 9.

A phase-group, mapping method, which is proposed here, would substantially speed such calculations while retaining the physics of rippled orbits, thermalization, and pitch-angle scattering.

ACKNOWLEDGEMENTS

The calculations described here were performed on the Cray computers at the National Magnetic Fusion Energy Computer Center at the Lawrence Livermore Laboratory, under contract to the U.S. Department of Energy. This research was sponsored by the Office of Fusion Energy, U.S. Department of Energy under contract AC-05-84OR21400 with Martin Marietta Energy Systems, Inc.

REFERENCES

[1] Putvinskii, S., Uckan, N.A., Borrass, K., et al., *Summary Report: ITER Alpha Particle Ripple Loss Meeting*, ITER-IL-PH-1-9-1 (8-10 March 1989) Garching, FRG

[2] Tani, K., Takizuka, T., Azumi, M., *Heat Load on the First Wall due to Ripple Loss of Alpha Particles*, ITER-IL-PH-1-9-J-1 (8-10 March 1989) presented at Garching meeting [1]

[3] White, R., *Ripple Induced Stochastic Alpha Particle Loss in ITER*, ITER-IL-PH-1-9-U-1 (8-10 March 1989) presented at Garching meeting [1]

[4] Konovalov, S.V., et al., *Alpha Particle Ripple Losses in ITER*, ITER-IL-PH-1-9-S-3 (8-10 March 1989) presented at Garching meeting [1]

[5] Hively, L.M., *TF-Ripple Losses from a Non-Circular Tokamak*, Nucl. Fusion **24** (1984) 779

[6] Hively, L.M., *Problems in Modeling Toroidal Field Ripple Loss of Fast Alphas from a Tokamak Reactor*, Fusion Technol. **13** (1988) 438

[7] Strickler, D.J., Peng, Y-K.M., Brown, T.G., *Equilibrium Field Coil Concepts for INTOR*, ORNL/TM-7746 (1981) Oak Ridge National Laboratory

[8] Uckan, N.A., and ITER Physics Group, *ITER Physics Design Guidelines*, ITER-TN-PH-8-7 (May 1989)

[9] Hively, L.M., *Convenient Computational Forms for Maxwellian Reactivities*, Nucl. Fusion **17** (1977) 873

[10] Lousteau, D.C., private communication (1988)

[11] Goldston, R.J., McCune, D.C., Towner, H.H., et al., *New Techniques for Calculating Heat and Particle Source Rates due to Neutral Beam Injection in Axisymmetric Tokamaks*, J. Comp. Phys. **43** (1981) 61

[12] Johnson, J.L., Reiman, A.H., *Self-Consistent, Three-Dimensional Equilibrium Effects on Tokamak Magnetic Field Ripple*, Nucl. Fusion **28** (1988) 1116

[13] Hively, L.M., Hirshman, S.P., Rome, J.A., *TF-Rippled Equilibrium for ITER*, 1989 International Sherwood Theory Conf. (San Antonio, Tx.) 3-5 April 1989

[14] Littlejohn, R.J., *A Guiding Center Hamiltonian: A New Approach*, J. Math. Phys. **20** (1979) 2445

[14] LITTLEJOHN, R.J., A Guiding Center Hamiltonian: A New Approach, J. Math. Phys. **20** (1979) 2445.

[15] GOLDSTON, R.J., TOWNER, H.H., Effects of Toroidal Field Ripple on Suprathermal Ions in Tokamak Plasmas, J. Plasma Phys. **26** (1981) 283.

[16] TANI, K., Japan Atomic Energy Research Institute, personal communication, 1988.

[17] UCKAN, N.A., Oak Ridge National Laboratory, personal communication, 1989.

[18] BOOZER, A.H., Enhanced Transport in Tokamaks due to Toroidal Ripple, Phys. Fluids **23** (1980) 2283.

[19] GOLOBOROD'KO, V.YA., KOLESNICHENK, YA.I., YAVORSKIJ, V.A., Alpha Particle Transport Processes in Tokamaks, Physica Scripta **T16** (1987) 46.

[20] GOLDSTON, R.J., WHITE, R.B., BOOZER, A.H., Confinement of High-Energy Trapped Particles in Tokamaks, Phys. Rev. Lett. **47** (1981) 647.

[21] WHITE, R.B., BOOZER, A.H., GOLDSTON, R., et al., Confinement in Toroidal Systems with Partially Destroy Magnetic Surfaces, IAEA-CN-41/T-3, In Plasma Physics and Controlled Nuclear Fusion Research (Proc. 9th Int. Conf. Baltimore, 1982), Vol. III, IAEA Vienna (1983) 391.

[22] ALBERT, J.M., BOOZER, A.H., A Bounce-Averaged Monte Carlo Collision Operator and Ripple Transport in a Tokamak, Phys. Fluids **31** (1988) 1809.

[23] ALBERT, J.M., BOOZER, A.H., Discrete Mappings and Resonant Ripple Transport in a Tokamak, Phys. Fluids **31** (1988) 1811.

[24] ALBERT, J.M., BOOZER, A.H., A Generalized Discrete Mapping Treatment of Nonresonant Ripple Transport in a Tokamak, Phys. Fluids **B1** (1989) 1335.

[25] ROME, J.A., PENG, Y-K.M., The Topology of Tokamak Orbits, Nucl. Fusion **19** (1979) 1193.

[26] HIVELY, L.M., MILEY, G.H., ROME, J.A., Fast-Ion Thermalization in Noncircular Tokamaks with Large Banana-Width Effects, Nucl. Fusion **21** (1981) 1431.

TABLE 1: Summary of Model

Model	Comments	Method
MHD Equilibrium	Finite beta, noncircular Pressure and safety factor specified	[7]
TF Ripple Field	8 straight-wire filaments per TF coil fit ripple data from Tani	[5-6] [16]
Net B-Field	2D equilibrium + TF ripple field	[5-6]
Plasma Profiles	Parabolic temperature for i/e Square-root parabolic density for i/e	[8]
Fusion Source	Numerical fit	[9]
Initial Conditions for Choosing Alphas	Uniform in poloidal flux coordinate Uniform in toroidal and poloidal angle Isotropic in velocity space Weight by source rate at birth point	[5-6]
Orbit Integration	4^{th} order Runga-Kutta of guiding center equation; time step = $2\pi R_0/Nv$; N=14	[5-6]
Time Scale Enhancement	1 for trapped ions, 200 for nontrapped ions	[5-6]
Loss to Wall	At elliptical wall (See Fig. 2)	[10]
Collisions	Slowing down, pitch angle scattering	[11]

TABLE 2: Filamentary wire parameters (see Fig. 2) for 14 TF coils, RMS fitting error = 5.75%

Parameter	Value (m)
R_1	2.322079
R_2	2.928964
R_3	7.495876
R_4	10.291451
Z_1	1.871173
Z_2	6.583143
Z_3	7.279346
Z_4	2.911957

TABLE 3: Summary of ITER (physics phase) parameters

Description	Symbol	Value	Comment(s)
Geometric center of plasma	R_0	5.8 m	
Minor radius of plasma	a	2.2 m	
Elongation	κ	2.13	
Triangularity	δ	0.51	
Toroidal field at R_0	B_0	5.0T	
Plasma current	I_{pl}	22.0 Ma	
Toroidal beta	β_t	6.7%	
Poloidal beta	β_p	1.0	
Major radius of poloidal null	R_{sep}	4.72 m	
Vertical offset of poloidal null	Z_{sep}	4.67 m	
Central temperature for i, e	T_0	20.0 keV	$T/T_0 = 1–0.99\ (r/a)^2$
Central density for electrons	n_0	$2.0\times10^{20} m^{-3}$	$n/n_0 = (1–0.99\ (r/a)^2)^{1/2}$ ions have same profile
Effective charge of ions	$\langle Z \rangle$	2.15	uniform impurity profile
Mass weighted effective charge	$[Z]$	0.44	uniform impurity profile
Plasma scrape-off thickness	s	0.15 m	